Virtual Flight Demonstration of the Stratospheric Dual-Aircraft Platform

W. A. Engblom[1]
Embry Riddle Aeronautical University, Daytona Beach, FL
R. K. Decker[2]
NASA Marshall Space Flight Center, Huntsville, AL

A baseline configuration for the dual-aircraft platform (DAP) concept is described and evaluated in a physics-based flight dynamics simulations for two month-long missions as a communications relay in the lower stratosphere above central Florida. The DAP features two unmanned aerial vehicles connected via a long adjustable cable which effectively sail back-and-forth using wind velocity gradients and solar energy. Detailed atmospheric profiles in the vicinity of 60,000-ft derived from archived data measured by the 50-Mhz Doppler Radar Wind Profiler at Cape Canaveral are used in the flight simulations. An overview of the novel guidance and flight control strategies are provided. The energy-usage of the baseline configuration during month-long stationkeeping missions (i.e., within 150-mile radius of downtown Orlando) is characterized and compared to that of a pure solar aircraft.

I. Introduction

A. Background

Aircraft platforms which could stationkeep in the stratosphere for years, referred to as *atmospheric satellites*, represent a long-standing, grand challenge to the aeronautics community, and have enormous potential societal and economic impact. Such platforms would diversify and expand surveillance capabilities (e.g., NASA's earth science missions) and communications bandwidth and availability (e.g., for underserved remote areas of the US, emergency communications), at a fraction of the cost of orbital satellite networks. Constellations of such platforms might potentially be integrated into the National Airspace System (NAS) to facilitate inter-aircraft communications or to support navigation or for aircraft surveillance. Constellations of such platforms could also improve communications and surveillance capabilities along major shipping lanes.

NASA and DARPA, and more recently industry, has funded development of aircraft which rely on solely solar power for propulsion, and the vehicles must accumulate and store a substantial amount of power during the day to operate at night. This is further compounded by the large variability of available solar energy during the year and the inability to point aircraft wings towards the sun to improve solar power capture. These factors result in severe limitations on the power that can be made available to the payload for communications, surveillance, etc.

B. Dual-Aircraft Platform

The Dual-Aircraft Platform (DAP), illustrated in Figure 1, is a concept for achieving a low-cost atmospheric satellite [1,2] which utilizes wind shear as the primary energy source, and has the potential to stationkeep for very long periods of time, providing substantial levels of power for its payload. DAP consists of two glider-like Unmanned Aerial Vehicles (UAVs) connected via a thin, strong cable which literally sails without propulsion, using levels of wind shear commonly found in lower Stratosphere (e.g., near 60,000-ft). The two aircraft are positioned at different altitudes, as far as 2,000-ft apart, to encounter substantially different wind velocities. The device operates similar in principle to a kite-surfer (see corner image) in which the upper aircraft, referred to as the *SAIL*, provides lift for both aircraft and aerodynamic thrust, while the lower aircraft, known as the *BOARD*, primarily provides an upwind force to keep the platform from drifting downwind (also like the keel on a sailboat). The aircraft derive power from solar cells, like a conventional solar aircraft, but also extract wind power using the propeller as a turbine when there is an excess of wind shear available. Power is needed to operate the avionics, flight controls, for intermittent use of propulsion, to retract cable when needed, and for the payload.

_____

[1] Professor, Departments of Mechanical and Aerospace Engineering, Associate Fellow AIAA
[2] Aerospace Technologist, Flight Vehicle Atmospheric Environments, Natural Environments Branch/EV44
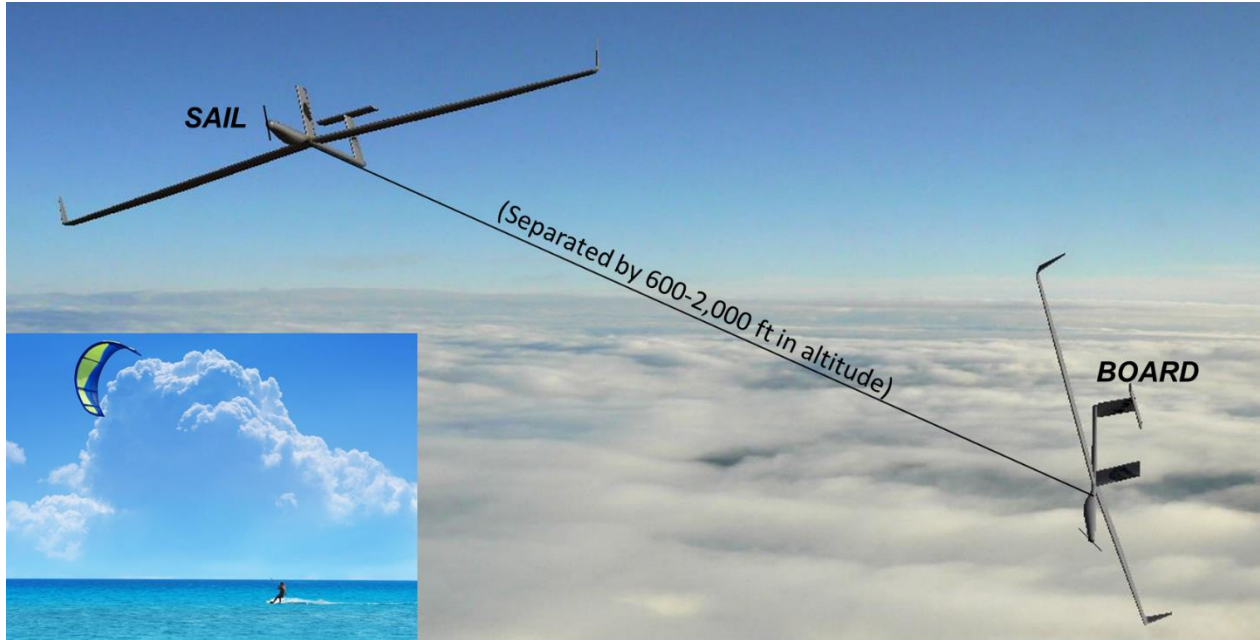
Figure 1. Dual-aircraft platform in sailing formation (aircraft graphics are scaled-up for clarity)

The theoretical basis of the DAP sailing concept has been described in detail [1]. A "guidance" software has been developed [1,2] which uses the atmospheric wind profile to determine the required DAP flight conditions to achieve sailing mode of flight. More specifically, the software determines the aircraft altitudes, platform's ground speed and heading, aircraft orientations, cable tension, and lateral (horizontal) spacing using a constrained non-linear optimization problem. Provided stringent targets for aerodynamic and structural performance are met, it has been shown theoretically that the device could achieve sailing conditions without propulsion at least 96% of the time within 60,000-70,000 ft.   This analysis depended on use of radiosonde data for various sites across the US mainland. However, radiosondes can drift significantly during ascent and provide limited spatial resolution of wind profiles with altitude. Consequently, a major focus of this effort was to utilize a more accurate and transient atmospheric model.

II. Methodology

A. Objectives

The primary objective of this effort is to compare the performance of a baseline DAP configuration versus a conventional solar aircraft for a specific mission as a communications platform. Two separate month-long flights during which the aircraft must remain within 150-miles of downtown Orlando (see Figure 2) are simulated such that an appropriate line-of-sight is maintained for communications with subscribers in the region. The upper aircraft is to provide power to a communications package which enables users below to connect to a cell tower. Details regarding the communications package configuration and its performance as a communications relay may be found in [3].

The main criteria of evaluation (i.e., comparison) are: i) daily net energy-usage, ii) daily solar energy capture, and iii) daily net energy made available to the onboard payload. A series of tasks were completed to meet this primary objective are listed below, and will be discussed in subsequent sections:

Principal Tasks

1. Refine aircraft configuration design to enhance sailing mode of flight performance.
2. Develop realistic transient atmospheric model using NASA KSC's 50 MHz Doppler Wind Profiler Radar.
3. Develop an effective *DAP* guidance strategy to define "waypoints" for the transient atmospheric model.
4. Develop the *DAP* flight control strategy to enable reliable long duration flight simulation.
5. Compile performance statistics for both DAP and a pure solar aircraft using flight simulation.

Figure 2. Station-keeping boundary of 150-miles around Orlando

B. DAP Aircraft Configuration

A "twin" DAP airframe configuration for the *SAIL* and *BOARD* is selected for this study, depicted in Figure 3. Although each aircraft has different roles, both aircraft must possess high aerodynamic efficiency (i.e., high lift-to-drag over a range of angles-of-attack) for the platform to sail within weak level of wind shear. Also, a twin configuration should reduce development and unit costs. The aircraft use a low-Reynolds number, highly cambered main wing airfoil (Eppler 397) with a deformable tailing edge (i.e., flaperons) to offer a relatively large glide-slope (i.e., aerodynamic efficiency) over a large range of angles-of-attack, which is vital for strong sailing performance. Further discussion on the aerodynamics performance is provided later in section G.

The size and mass targets listed on Figure 3 is assumed to be attainable based on comparison to the Zephry 7 stratospheric solar aircraft (i.e., DAP @ 0.61 lb/sqft wing loading vs. Zephyr 7 @ 0.36 lb/sqft), although no detailed structural design has been conducted. This aircraft structure would need to be heavier and more structurally stiff than a conventional solar aircraft to handle the 3-g wing loads that are typical of the sailing mode. However, DAP would require a lighter energy storage system for overnight operations due to use of sailing mode of flight overnight.

The aircraft wings are assumed 80% covered in solar film on both upper and lower surfaces (unlike a conventional solar aircraft which could only benefit from treatment of the upper surface). Although 20% efficient solar energy capture is assumed, the losses associated with storing/retrieving energy from the batteries, and converting the energy into usable propeller energy is reflected in the assumption here of an *effective* solar capture efficiency of 15%.

C. Mast with Laterons

The fixed "mast" surface atop the main wing with moveable "lateron" control surface is unorthodox but found from flight simulation to enable smoother *transitions* between sailing (i.e., high cable tension) and standard cruise (i.e., low cable tension; near level flight) modes of operation. It is found that this control surface enables faster lateral (y-directed) force response than the conventional method of rolling the aircraft, which has to overcome a relatively large roll moment of inertia. It is also desirable to avoid use of roll to minimize potential for cable to aircraft impingement. However, the potentially significant aerodynamic interference of the wake from this surface with the vertical stabilizer has been neglected in this study.
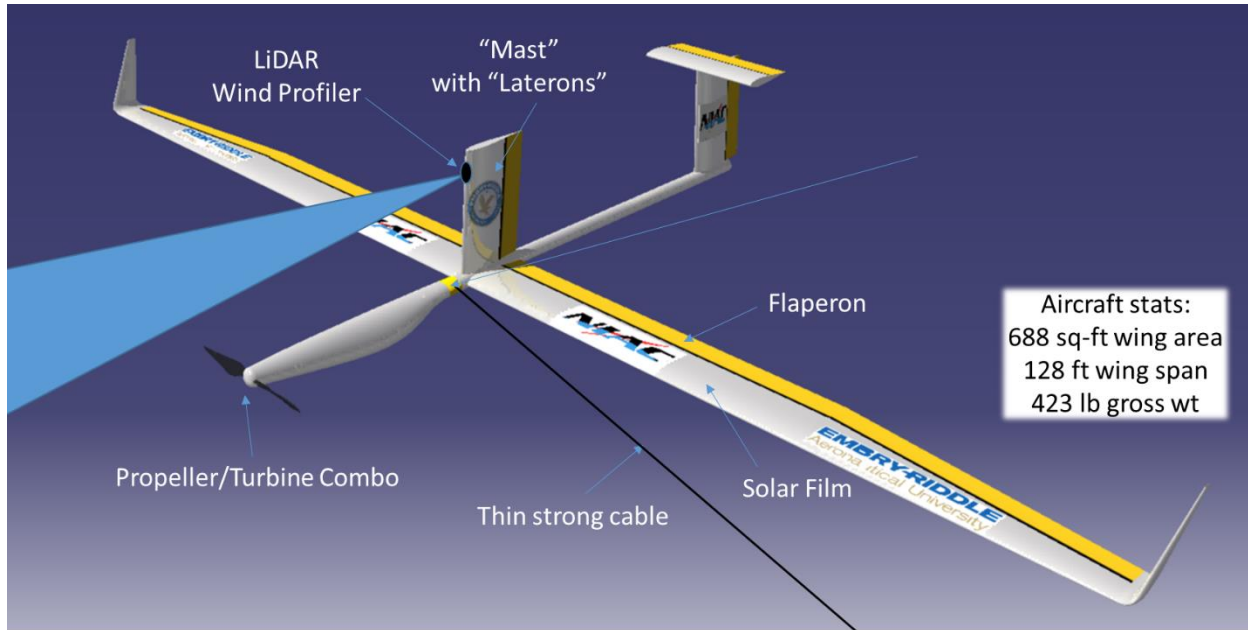
3

Figure 3. Baseline configuration for the dual-aircraft platform

Figure 3. Stratospheric DAP aircraft configuration used for flight simulations

D. LiDAR Wind Profiler

A miniaturized LiDAR wind profiler is also positioned within the "mast" for an unobstructed view to *forecast* the incoming wind shear. Early efforts at long-term flight simulations with small to no forecasting (i.e., no advance knowledge of the incoming wind conditions) led to unacceptable performance. LiDAR is assumed to obtain profiles 3-5 minutes ahead of the current DAP position (i.e., approximately 4 km ahead based on typical airspeed) and roughly 1 km above and below the aircraft altitudes (i.e., assuming a 30° conical region is measured).

Advancement in LiDAR wind profiling technology at NASA includes successful demonstration of onboard LiDAR wind profilers. For example, NASA GSFC's TWiLiTE program demonstrated use of an onboard Doppler wind profiler using the NASA ER-2 high altitude aircraft [4], as well as on Global Hawk. NASA Langley's Doppler Aerosol Wind (DAWN) program [5] has demonstrated high-accuracy LiDAR-based wind profiling on the DC-8 aircraft. However, the weight and power usage of these systems are far too large for use on DAP.

NASA Langley's Laser Remote Sensing Branch has demonstrated that LiDAR systems for navigation can be significantly miniaturized [6]. Figure 4 below shows a NASA Langley's 2012 prototype miniaturized LiDAR system chassis for navigation, weighing less than 16.4 kg and requiring only 95 W of power and having range of 2.5 km. A much lighter (10 kg), more energy efficient (85 W), and longer range (4 km) LiDAR chassis is to be completed in 2016 (shown to the right). Although these LiDAR systems measure hard target velocity, and are not directly applicable to the DAP, it is speculated that with sufficient investment, a miniaturized LiDAR-based wind profiler could be developed for DAP which meets similar specifications for weight, power, and range.

Figure 4. Miniaturized LiDAR chassis developed at NASA Langley in 2012 and 2016

E. Cable Connection System

The cable connection system is configured to accommodate retraction/extension of the cable, and avoid cable-to-aircraft impingement. The cable material is currently chosen as Dyneema, an ultra-high-molecular-weight polyethylene fiber, as depicted in Figure 5. An off-the-shelf 3.0-mm diameter braided cable like that shown in Figure 5 (left) provides a breaking strength of 2700 lbf, according to the vendor, which is several factors more than the platform can create during cruise at maximum lift (i.e., allows a safety factor of more than 3). A strong dynamic component (i.e., the aircraft move apart at a relative speed of roughly 20 knots) would be sufficient to break the cable, but is deemed unlikely. For subsequent analysis it is assumed that the DAP's cable offers double the maximum allowable tensile stress (and modulus of elasticity) of the aforementioned off-the-shelf cable. Consequently, the cable is assumed to be 2.1-mm in diameter while maintaining a safety factor of 3.0.

The *SAIL* aircraft trajectory is constrained to fly ahead of the *BOARD* to avoid cable-to-aircraft impingement of the *BOARD*. The center of gravity (cg) of the aircraft is located just in front of the main wing to permit connection of the cable directly to the cg (see gold cylinder), which minimizes aircraft-to-aircraft induced moments. The forward position of the CG results in an undesirable but acceptable loss of aerodynamic efficiency due to the need for a larger horizontal stabilizer and/or tail boom. The gold cylinder on the *SAIL* aircraft (see Figure 3) includes an electrically-powered "fishing-reel" (winch) mechanism to adjust cable length in-flight. The gold cylinder on the *BOARD* contains a "roller-bearing" mechanism to permit free aircraft rotation while connected to the *SAIL*, as depicted in Figure 5 (right). The outer section of this mechanism is free to rotate as the *BOARD* rolls.

Figure 5. Elements from Cable Connection System. Dyneema Cable (left);
Tapered Roller Bearing on *BOARD* (right)

F. Propulsion/Turbine System

The electric propulsion system is configured to include 1.5 meter long blades electric propeller blades (i.e., 3 meter diameter system) which are extendible/retractable to minimize drag during cruise. These blades and are also unconventionally to be used to extract wind power in a "turbine mode" via variable geometry (twist and pitch). Alternatively, the propeller blades may be retracted while another pair of turbine blades are extended, from the same shaft. A propeller-driven sport aircraft that can extract energy during descent has been developed and demonstrated by Pipestral in Slovenia. It is speculated that a similar device could be developed for use in the lower stratosphere.

For the purposes of analysis, a simple 1-D actuator model is used to estimate the power required to achieve a specified thrust (propeller mode) or drag (turbine mode). A maximum thrust of 12.5 kW is selected based on flight

simulation. Moderately high propeller and turbine kinetic energy efficiencies of 75% and 25%, respectively, are assumed.

G. Aerodynamics Assessment

An important aspect of developing a new aircraft configuration is to produce credible aerodynamics performance data for use in the flight simulations. *XFOIL* is used to evaluate 2-D airfoil performance, which is later adjusted for 3-D finite-wing effects (e.g., adding induced drag). The effects of control surfaces and the dynamic stability are introduced using linearized aerodynamics coefficients obtained from a vortex lattice method (VLM) solver, *Tornado*. Both software are distributed under a GNU-general Public License. The profile and skin friction drag coefficients for the fuselage are estimated based on typical glider values. The maximum lift-to-drag of the baseline configuration is approximately 35 at a typical sailing flight Reynolds number of 500,000. For purpose of simulation, limits are imposed on control surface deflection, deflection rates, as well on the thrust response.

A more detailed aerodynamic characterization is unwarranted at this early stage in development. However, it should be emphasized that the guidance software requires accurate characterization of the aircraft aerodynamics to determine sailing mode flight conditions. Consequently, for practical implementation, the aircraft aerodynamics would need to be well characterized apriori.

H. Atmospheric Model derived from KSC Doppler Radar Wind Profiler

A crucial element of the study was for NASA-MSFC to develop a high fidelity transient atmospheric model possible for long-duration flight simulations near 60,000 feet (18.3 km). Empirical databases exist to estimate wind profiles for a given time of the year, like the Earth Global Reference Atmospheric Model offered by NASA Marshall Space Flight Center. These databases offer accurate statistical representations of the winds at a given altitude and time of year. However, we opted instead to build a unique, high-fidelity model based on high-temporal frequency atmospheric profiles measured by the 50-MHz Doppler Radar Wind Profiler (DRWP) over KSC.

DRWP-measured wind profiles over KSC coupled with simultaneous weather balloon thermodynamics observations are utilized to produce two separate long duration transient atmospheric environments which the DAP would encounter at flight altitudes between 15-18.5 km (i.e., the 30 and 39 day intervals listed below). Winter season cases were selected for DAP performance assessments as the winter season in central Florida exhibits the most variability/dynamic environment annually. These specific time intervals were primarily chosen to minimize the temporal gaps in the DRWP datasets. These cases were also representative of the upper atmospheric climatology over central Florida.

     i. February 10th to March 11th (2011) – 30 days
    ii. January 17th to February 24th (2006) – 39 days

Although these datasets represent a dynamic atmospheric wind model, the effect of high frequency gusts is not captured due to temporal averaging in 3 to 5 minute intervals. To capture the effect of higher frequency gusts, integration of a standard wind turbulence models (e.g., Dryden or Von Karman) is possible, but has been neglected for this study.

Since these two datasets comprise only a small sample of the upper atmospheric environment, statistics from these cases were compared against an independent database to determine how the cases compared against climatology. The mean of all the variables for each case were calculated and plotted against the mean, "mean + 3-sigma" and "mean – 3-sigma" February climatology from the CCAFS RRA. The data was plotted against the month of February only since it contained the majority number of profiles for both cases. Wind speed and direction data were converted to U and V components. The mean wind components for both datasets closely resembled the RRA monthly mean as shown in Figures 6. Likewise the thermodynamic data closely followed the RRA monthly mean for the two datasets. These results verify these cases are valid representations of the upper atmospheric environment over central Florida.
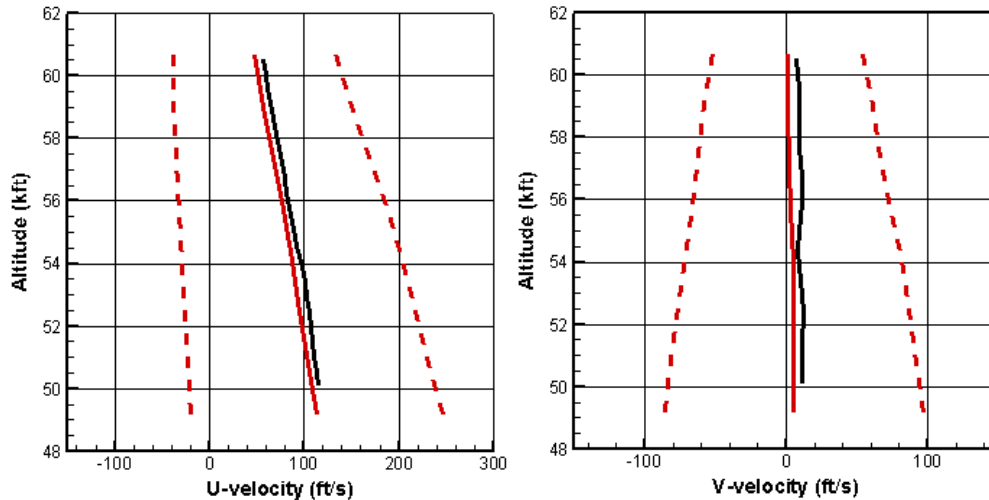
Figure 6. Mean U- (left) and V-components (right) from 2006 dataset represented by the black solid line. Red solid line is the representative mean wind component from 2013 CCAFS RRA. Red dashed lines are the "mean – 3-sigma" and "mean + 3-sigma" curves.
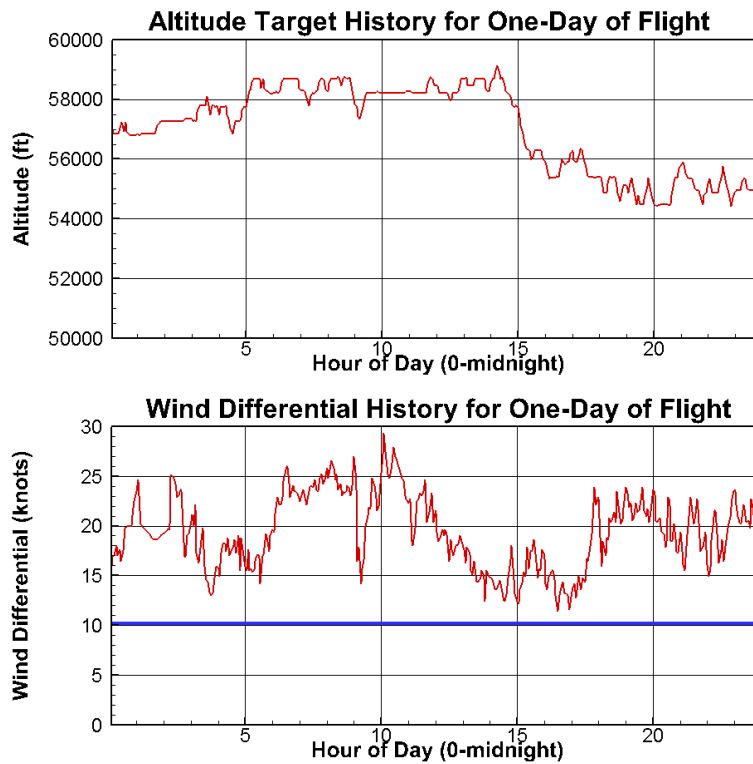

Figure 7. *SAIL* altitude history and corresponding wind differential across platform during 24-hour period

A cursory examination of the atmospheric datasets show that sufficient levels of wind shear to enable the DAP sailing mode of operation are persistently available. Figure 7 (top) shows a hypothetical altitude history over the first 24-hour period of the aforementioned 39 day data set. Despite trajectory restrictions of a constant 2,000 ft altitude separation between the *SAIL* and *BOARD* aircraft, and a limit on ascent/descent rates of 2 ft/sec, the platform would be able to "find" more than sufficient wind shear (i.e., > 10 knots wind differential) to permit sailing for the entire 24-hour period as shown in Figure 7 (bottom). Over the 39 day dataset, the platform remains above this 10 knot differential for 93% of the duration. This assumes that the aircraft can "forecast" the wind profiles 3-5 minutes ahead using an onboard LiDAR wind profiler. Note that if sufficient wind shear is present, propulsion is not necessarily

needed to ascend, and wind energy may be extracted by using the propeller as a wind turbine, reducing the net energy required to remain aloft. Although the DAP trajectory determination is not this simple, this examination strongly suggests that persistent wind shear is available to support the sailing mode of operation.

H. DAP Guidance Software (Sailing Flight Operations)

DAP guidance software originally demonstrated in [1] has been refined to support long-term flight simulations using the aforementioned DAP configuration and transient atmospheric models. This software is written in FORTRAN90 and uses a constrained nonlinear optimization technique to determine the optimal aircraft altitudes, speed, heading, orientation, and lateral spacing for sailing mode in a given atmospheric profile. Specifically, the sailing mode involves cruise at constant platform speed and heading – a "pseudo-steady soaring" mode of flight. Unlike conventional waypoints that consist of target positions versus time (i.e., a trajectory), the DAP waypoints represent a more complex state of ten (10) variables necessary to achieve sailing mode of flight, including:

- Z_S (*SAIL* altitude)
- Z_B (*BOARD* altitude)
- V, γ (platform ground speed and heading from North)
- α_S, ϕ_S (*SAIL* angle-of-attack and roll angles)
- α_B, ϕ_B (*BOARD* angle-of-attack and roll angles)
- X_{SB} (*SAIL* distance from *BOARD* in *X*, North)
- Y_{SB} (*SAIL* distance from *BOARD* in *Y*, East)

The sideslip angle is zero as a consequence of the Euler angle rotation sequence of yaw-roll-pitch, where the yaw rotation puts the aircraft directly into the relative horizontal wind. If sailing is not possible, a more conventional yaw-pitch-roll sequence is used with an additional explicit constraint to limit the sideslip angle to a finite angle.

This software calculate these target flight conditions (or "waypoints") every 3-5 minutes to correspond with the new time-varying atmospheric model profiles developed by NASA-MSFC. A series of constraints are imposed in the optimization technique to produce smooth variation in these waypoints to improve flight controllability and minimize energy usage. Additional constraints are needed to promote aircraft safety, including, but not limited to:

- Altitude range limits (50,000 – 62,000 feet)
- Maximum allowable dynamic pressure (structural limit)
- Maximum allowable cable tension (limited by tensile strength and safety factor)
- Maximum extended cable length (cable length limit)
- Minimum allowable angle of cable relative to *SAIL* yaw plane (avoid aircraft-cable contact)
- Range of allowable angle of cable relative to *BOARD* roll plane (avoid aircraft-cable contact)
- Minimum allowable tether tension (must always be positive to be in tension; avoid knots)
- Range of allowable angle-of-attack (avoid stall)

This software currently identifies target platform state conditions that permit sailing mode of flight (i.e., without propulsion) for greater than 90% of the duration of both of the 30+ day atmospheric models. When the sailing mode of operation is not available, the guidance software establishes a waypoint for which the use of thrust is minimized.

Occasionally the software requires significant computational effort to complete the optimization process. It is concluded that waypoint solutions will likely need to be generated and tabulated for a wide range of potential atmospheric conditions and stored onboard the aircraft for quick retrieval.

I. DAP Guidance Software (Transition Flight Operations)

The guidance software will require DAP to make "transitions" between the sailing flight mode and a formation flight mode. For example, DAP must intermittently complete near 180° turns to fly back towards the center of the service area (i.e., to stationkeep). Before a turn the platform must transition from sailing mode to formation flight mode, and after the turn, the platform must transition back to sailing mode. Also, when the platform must make a considerable change in altitude (or even in lateral spacing), the platform will need to transition into formation flight before making these changes in the flight conditions, and then transition back to sailing mode when appropriate.

These transitions are not trivial. First, the cable tension is relatively large during sailing flight mode and nearly slack during formation flight. The *BOARD* aircraft often operates at roll angles of approximately 90° while sailing,

but must regain level flight when in formation. Additionally, there is potential risk for cable-to-aircraft impingement during these transitions if not sufficiently controlled. These transitions represent a significant controls challenge. Consequently, a smooth and low-risk style of transition is highly desirable.

The FORTRAN-based guidance software currently creates a series of "mini-waypoints" to support these transition maneuvers which takes a few seconds of real time to compute. These waypoints represent pseudo-steady flight conditions that enable a smooth and safe transition. The cable is connected to the *BOARD* aircraft just ahead of the main wing to permit free rotation via a "roller-bearing" mechanism (see Figure 5). Flight simulations show this style of transition to be relatively smooth and easy to control. The additional use of the mast and lateron control surface permits faster and safer transitions, but successful transition without the mast surface have been demonstrated in flight simulations.

Figure 8 provides a snapshot of before and after a "transition" simulation from a standard flight formation mode (top) to the sailing flight mode (bottom). Note that the tension in the cable (at the *SAIL* attach point) is relatively weak (~70 lbf and slackness is evident) while the aircraft move in formation in effectively steady, level horizontal flight. The aircraft are pointed into their respective relative winds. The *SAIL* appears larger since it is at a higher altitude, and the aircraft images are only placeholders for the actual shape. The tension and tightness in the cable grows steadily as the aircraft reach the sailing flight condition, to maximum levels of nearly 600 lbf in this case. It is important to note that such a transition has not been done in real world flight to our knowledge, but this physics-based simulation suggests that it can be done without the aircraft losing control or impinging the cable.
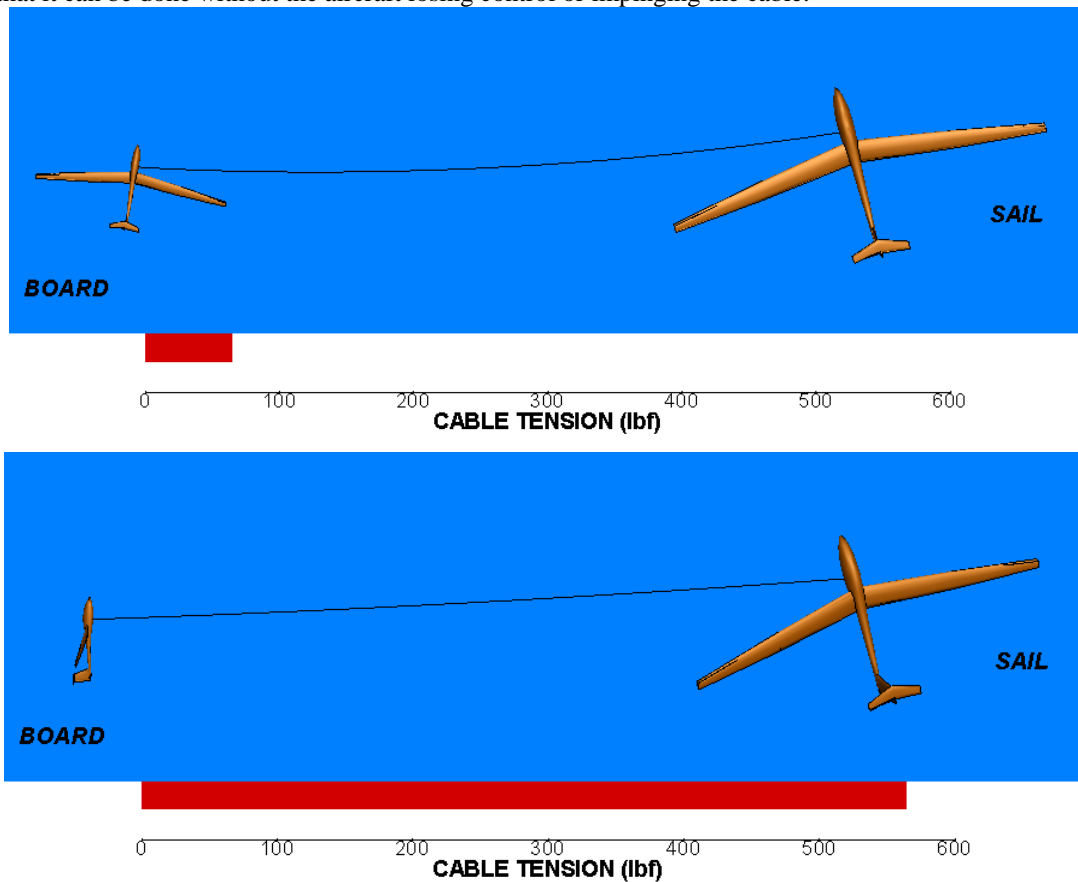

Figure 8. Start and end images from animation of the transition maneuver
(from "standard" to "sailing" flight modes)

J. DAP Flight Controls Algorithm

The flight controls logic uses an unconventional set of control law and a fixed-parameter linear control approach. Quaternion-error based attitude control develop by Wie [7], traditionally used by spacecraft, is used to reach target quaternions which correspond to target Euler angles (α, β, γ). Use of spacecraft control laws was chosen considering

that the aircraft attitudes, especially the *BOARD*, vary a great deal more than conventional aircraft. Conventionally, the aircraft ailerons, rudder, and elevator provide the control torques.

The flight controls logic also uses inertial velocity errors (and relative position errors of the two aircraft) as the basis for reaching a target velocity and relative position. The inertial, 3-D control forces required by each aircraft are transformed into the body frame for each aircraft. The axial thrust, laterons, and flaperons provide the X-, Y-, and Z-body frame velocity and position control, respectively.

PID controllers have been tuned for this six degree-of-freedom controls approach, and have enabled successful completion of flight simulation using the long duration (i.e., 30 and 39 day) atmospheric data sets. Conventional aircraft use roll adjustments to alter lateral speed and position, but this approach was not investigated in this study to avoid increasing the potential for cable-to-aircraft impingement. The controls logic also contains special provisions for when the aircraft must make a significant climb or descent while sailing. Although long term flight simulation is enabled with this algorithm, adaptive controllers to replace the PID controllers may be warranted.

K. DAP Flight Simulator

DAP's flight simulator is based on the LaRCsim flight model, originally developed at NASA Langley [8]. This model is available within FlightGear, which has been released under the terms of the GNU General Public License. The portion of the flight model which pertains to the 6-DOF dynamics of a rigid aircraft, originally written in C, has been converted to FORTRAN90, and modified to permit simulation of two aircraft simultaneously, as well as integration of the aforementioned controls logic.

A multi-degree-of-freedom segmented cable model is also integrated into the simulator to handle the cable dynamics and interactions between the two aircraft. The cable is typically simulated as twenty equal length segments. Longitudinal wave speed propagation along the cable has been verified to approximate the square-root of the specific modulus of elasticity:

$$V = \sqrt{E_o/\rho} \qquad (1)$$

Based on vendor data for Dyneema, the wave speed is roughly 10 km/s when the cable is in tension. This high wave speed is essential for the aircraft to operate synergistically.

The aerodynamic forces on the cable are a major limitation of sailing performance. These forces are modeled based on Hoerner's method [9] for a cylinder in crossflow. Based on the low Reynolds numbers involved, a normal force coefficient of 1.0 is imposed for the cross flow acting on each segment along the cable, and a skin friction coefficient of 0.02 is imposed along the wetted area of each segment along the cable.

L. Daily Energy Usage Estimates

Energy usage by the propulsion system for the *SAIL* and *BOARD* aircraft during long duration flight over central Florida are derived from the time-accurate flight simulation results. As previously mentioned, the guidance algorithm defines waypoints every 3-5 minutes which maintain the sailing flight mode and typically do not require "drastic" changes to the platform flight conditions. When sailing conditions are not possible, a minimal level of thrust is imposed by the waypoint conditions. The flight time intervals associated with the aforementioned waypoints account for typically greater than 95% of a given day. The energy usage during these time intervals is simply integrated based on the thrust used (or created in turbine mode) for each one-second in the flight simulation. As mentioned previously, 1-D actuator models are used to derive the power required as a function of thrust (or drag) for each mode.

The remaining portion of the flight duration that involves "drastic" changes to the flight conditions is not simulated in time. For example, the platform may need to make a large altitude change of 1000 ft over the next 3 minutes to find better wind shear. More commonly, the aircraft must turn around in formation to remain within the 150-mile stationkeeping limit. For these events, the propulsive energy usage is estimated based on the power required to climb/descend, the duration, and using an assumed formation flight glide slope of 20. So, the long term flight simulations "skip" over these events.

The power required to operate the onboard LiDAR wind profiler, and the power needed to retract the cable during flight, are addressed to provide a more fair comparison with a pure solar aircraft. Based on correspondence with NASA Langley's Laser Remote Sensing Branch, a 100-W power continuous power usage for a miniaturized LiDAR is a reasonable goal. Based on a typical retraction rate of 2 cm/s (from flight simulation results) at a typical cable tension during sailing of 650 lbf, and a mechanical efficiency of 80%, the power required to retract the cable is approximately 70 W. This power may be supplied by an onboard electric winch, or possibly driven off the propulsion system's electric motor. Cable extension occurs at similar rates in the flight simulations but the energy cost is neglected as small. The energy required to actuate control surfaces and run onboard avionics is also neglected.

III. Results

The results from two long duration flight simulations of 30 and 39 days are summarized. The 30 day flight simulation was used to focus on developing a guidance and flight control strategy that results in low propulsive energy usage by the DAP relative to a pure solar aircraft flying solo. The 39 day flight simulation was used to include consideration of solar energy capture during the flight simulations. Consequently, the net energy remaining for the onboard payload is also evaluated with the 39 day flight simulation results.

For the sake of comparison, the pure solar aircraft, *SOLAR*, is assumed to have the same weight and wing area as the DAP aircraft. SOLAR flies solo with wings level, and at a near peak lift-to-drag ratio of 35 at 60,000 feet. Consequently, the daily net energy usage by propulsion for *SOLAR* is a constant.

A. DAP Propulsive Energy Usage for 30-Day Flight

Figure 9 (left) shows the daily energy usage by the propulsion system for the *SAIL*, *BOARD*, and *SOLAR* aircraft for the 30 day atmospheric model described in Section IIH. Twelve days involve negative net energy usage, and all of the days require less than one-third the energy required by an identical aircraft (i.e., size, weight, etc.) flying solo as a conventional SOLAR aircraft. Excess wind energy is often available, and the propulsion system can create negative thrust (i.e., drag), using the wind turbine mode, to maintain steady sailing conditions.   As expected, this extra wind shear resource is not consistent day-to-day.

Figure 9 (right) shows the daily energy usage for the same 30 day flight if the wind turbine mode is not permitted. That is, the aircraft would need to create drag using spoilers or other means. Interestingly, the daily energy becomes more consistent from day-to-day and the maximum daily usage is unaffected. Still, DAP requires less than half the energy required by *SOLAR*.

Figures 9 is the result of several iterations on the guidance logic to find the approach which leads to minimal daily net energy usage. It should be emphasized that the guidance software makes no attempt to consider solar energy capture. Consequently, there are several days during which one or both of the DAP aircraft capture much less solar energy than the *SOLAR* aircraft.   Nevertheless, these results suggest that propulsive energy requirements can potentially be significantly reduced using the sailing mode of operation.
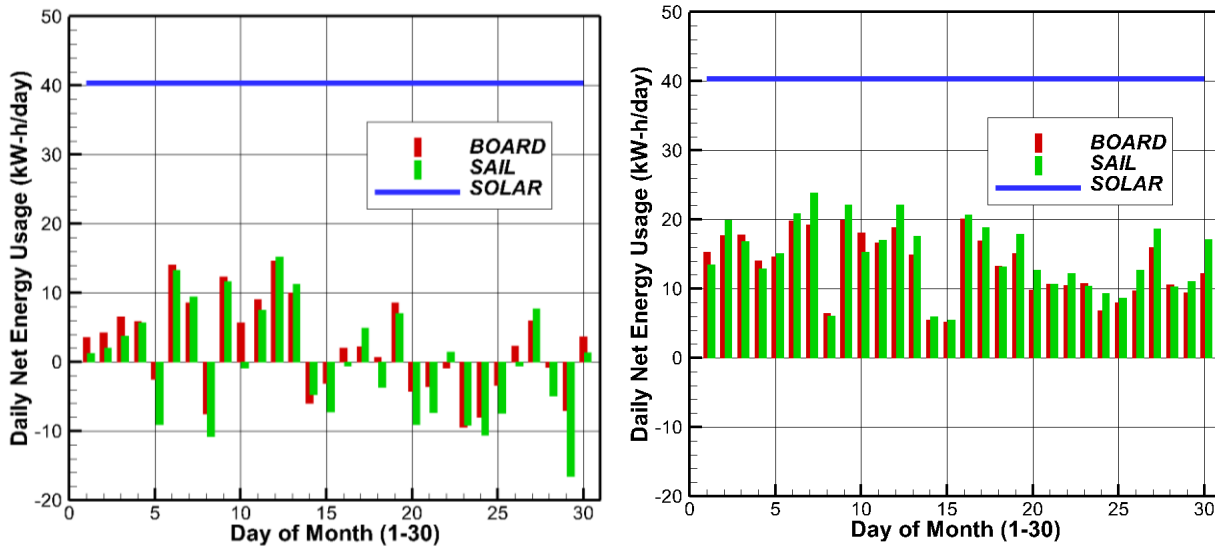

Figure 9. Daily energy usage by DAP aircraft compared to pure solar aircraft over 30 days
with turbine mode active (left), turbine mode inactive (right)

B. DAP Propulsive Energy Usage and Solar Energy Capture for 39-Day Flight

Figures 10 (left) shows the daily energy usage by the propulsion system for the *SAIL*, *BOARD*, and *SOLAR* aircraft for the 39 day atmospheric model when the turbine mode is active. In this simulation, the DAP aircraft operate in standard formation flight mode (i.e., fly with level wings) during the mid-day hours when the solar energy capture of the *SAIL* aircraft would be improved by flying level. This is the only major change made to the guidance logic relative

to the previous 30 day flight. Consequently, the net propulsion energy usage by DAP tends to be larger compared to the results provided in Figure 9 for which no attempt to improve mid-day solar energy capture is made.
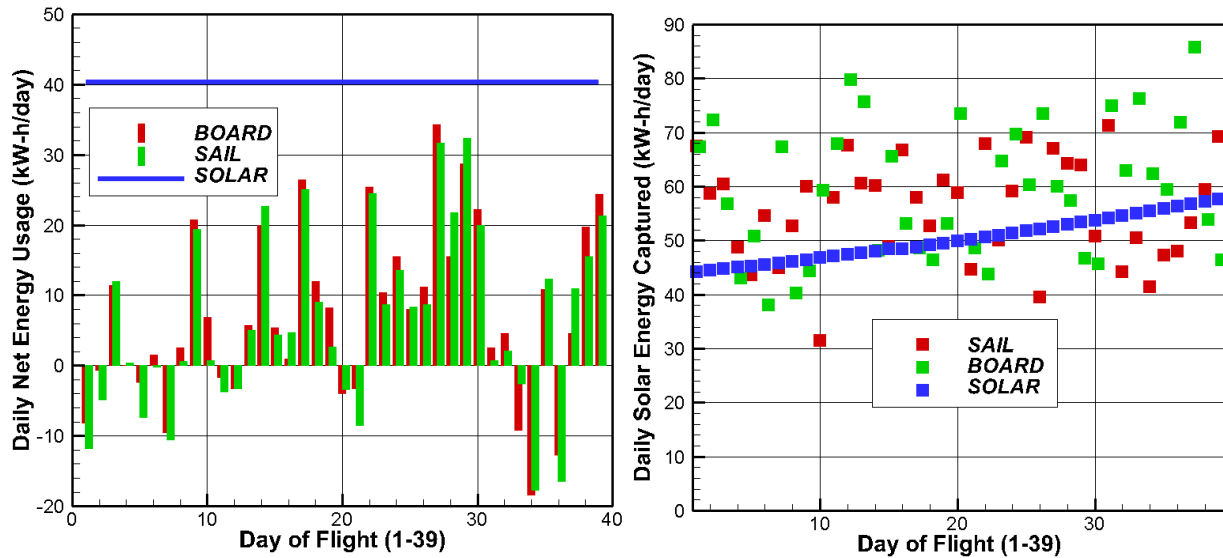

Figure 10. Daily energy usage and solar energy capture by DAP aircraft
compared to pure solar aircraft over 39 days

Figure 10 (right) summarizes the solar energy capture for the *SAIL* and *BOARD* compared to the conventional *SOLAR* option. Because the DAP aircraft do not fly wings level, the use of solar film/cells on both upper and lower surfaces of the wings results in typically much better solar energy capture for DAP than the pure solar aircraft. Note that the DAP guidance software makes no attempt to improve solar energy input while sailing (i.e., orient the aircraft to improve solar capture), and such an approach could lead to more consistently large solar energy capture.

Figure 11 summarizes the daily net energy available to the payload (i.e., the solar energy input minus the propulsive energy usage) for the DAP versus two *SOLAR* aircraft. This comparison assumes the *SAIL* and *BOARD* could transmit/share power along a thin electrical wire embedded within the cable. *The DAP is predicted to consistently provide a great deal more energy to the payload than the two SOLAR aircraft.* This comparison would become more stark near the winter solstice when available solar energy is at its minimum (i.e., one month prior to this timeframe). From Figure 11 one could project that the pure solar aircraft would not be able to support a payload in the vicinity of that timeframe.
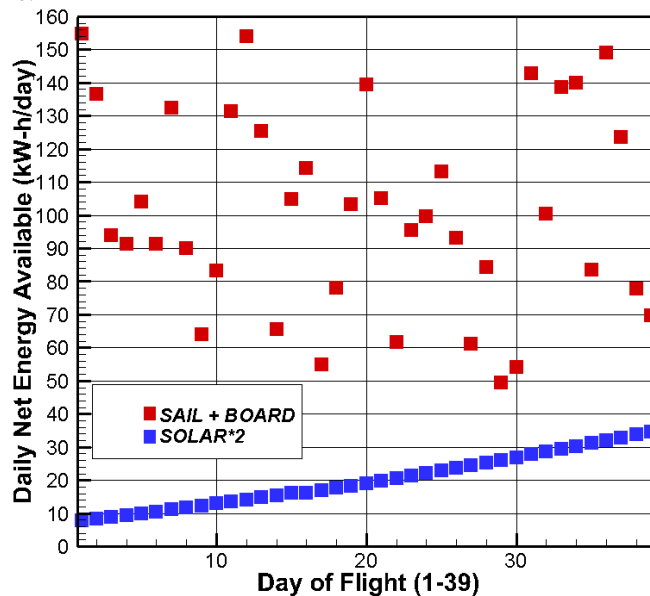

Figure 11. Daily net energy available to the payload (DAP vs. SOLAR)

C. DAP Trajectory Characteristics

Figure 12 illustrates histories of the *SAIL* (red) and *BOARD* (blue) aircraft altitudes, roll angle, and local wind speed and direction for one characteristic day (i.e., day #36 in the 2006 dataset). This day resulted in negative net propulsive energy usage due to persistently available wind shear. Two large altitude changes in the vicinity of 60,000 feet are made during the day (i.e., in the 2nd and 14th hour), and these coincide with nearly 180° turns made to remain within the 150-mile stationkeeping radius. Roll orientations switch abruptly between positive and negative values each time the aircraft makes a nearly 180° turn, of which four are evident. Note that the roll orientation of the *SAIL* is always less than that of the *BOARD*, as expected for sailing mode of flight. Figure 12 also depicts the wind conditions encountered by the platform. The local (inertial) wind speed histories indicate a nearly persistent wind differential of 10 or more knots between the aircraft over the course of the day. The local (inertial) wind direction histories indicates that a persistent westerly wind which varies only about 40° over the day.
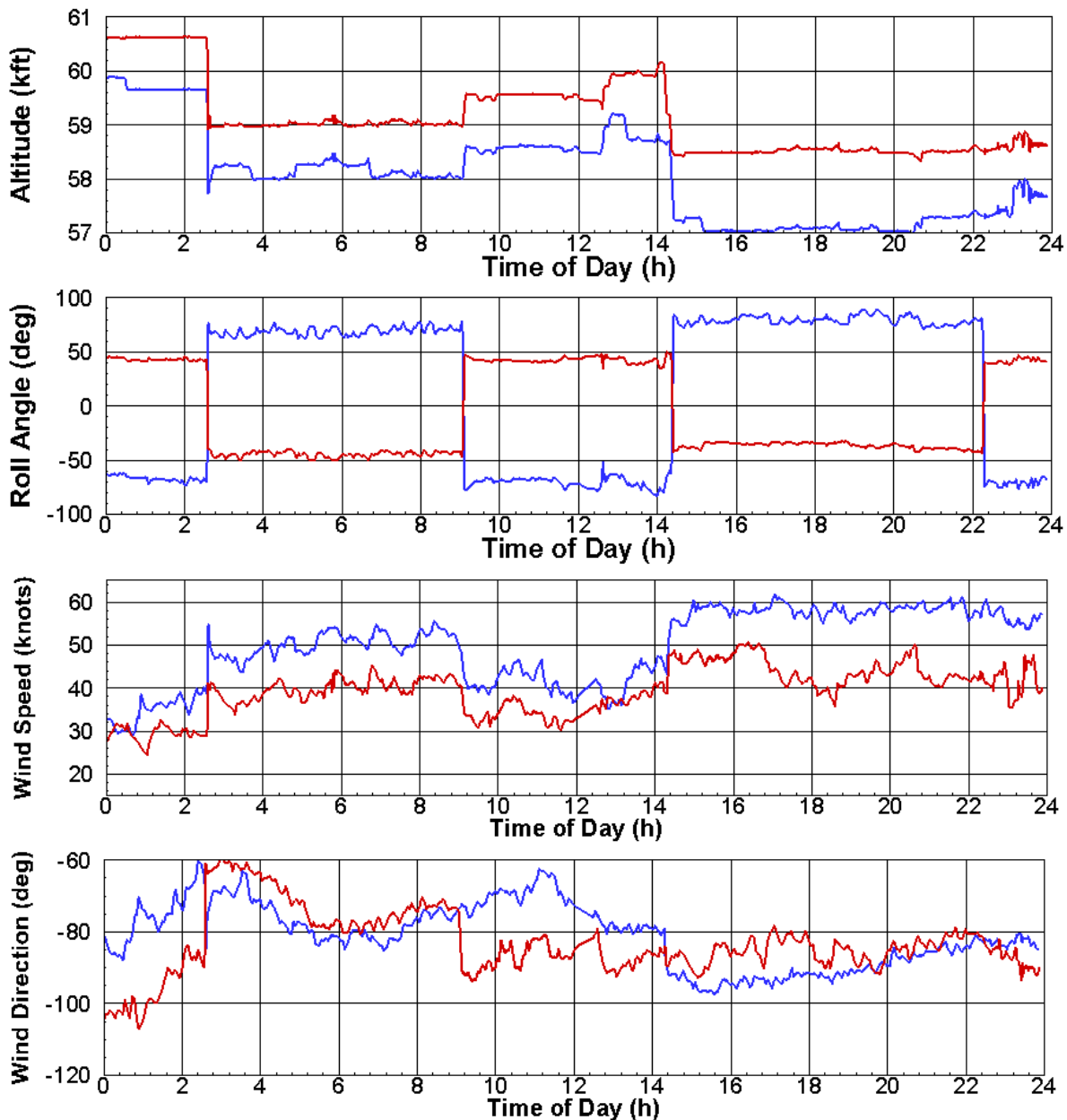

Figure 12. Trajectory altitude, roll orientation, and local wind speed and direction during day #36

Figure 13 illustrates histories of the aircraft yaw orientation (i.e., of fuselage relative to due North), the platform heading (i.e., relative to due North), and ground speed. The yaw orientation history shows that the aircraft are always pointed with some easterly component. The heading history, which is nearly identical for both aircraft, shows that the platform is moving primarily north (0°) and south (±180°) but has some drift west or east.   Note that near due south the heading angle can oscillate between extremes. Also, as the ground speed approaches zero (e.g., near the 16th hour), the heading angle becomes ambiguous.   So, the platform can remain in nearly one position in space. Also, the platform can drift downwind (i.e., westerly) while facing easterly. These flight trajectory characteristics are analogous to a sail boat tacking back and forth against a strong wind, and not travelling far upwind.
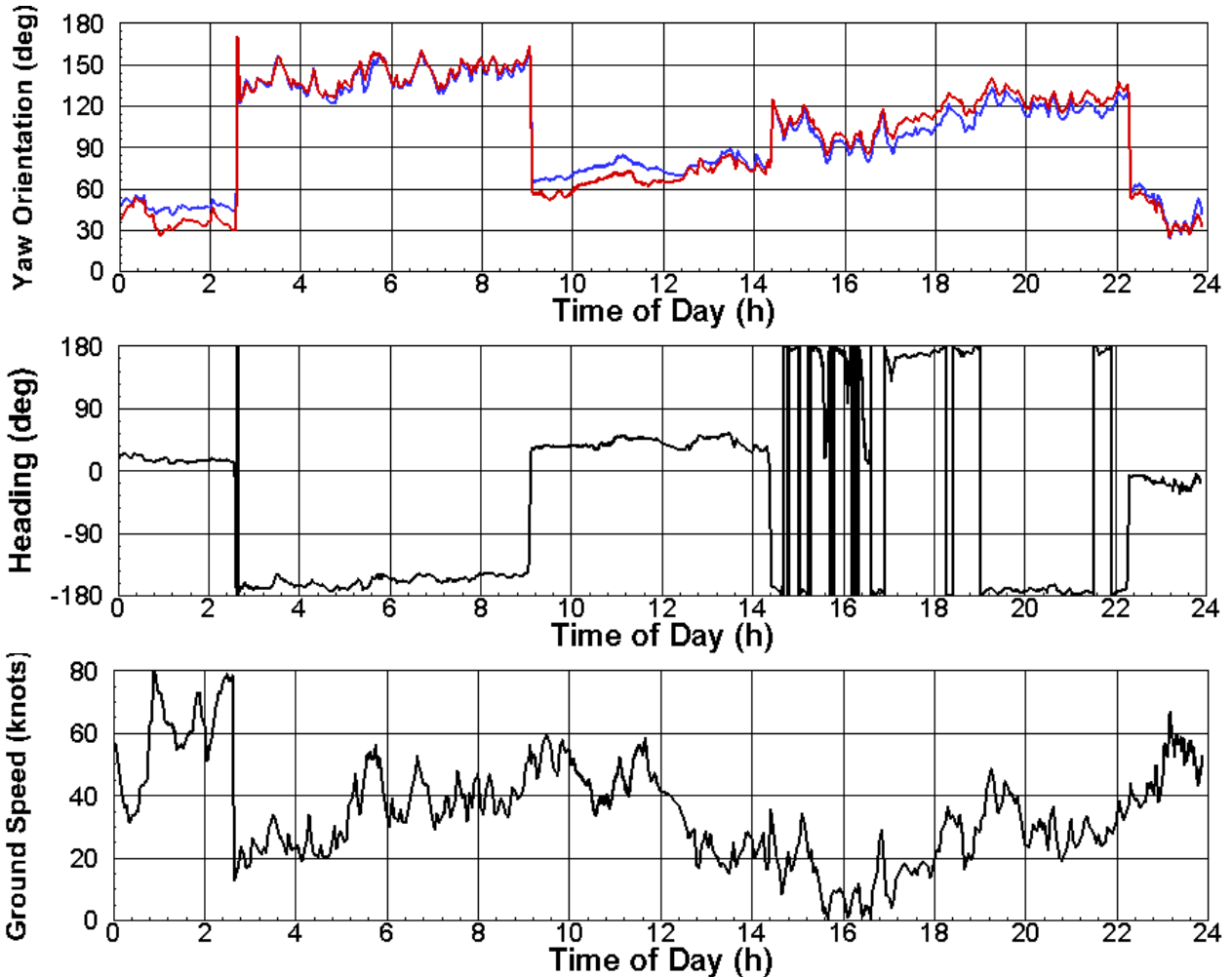

Figure 13. Trajectory yaw orientation, heading, and ground speed histories during day #36

Figure 14 illustrates corresponding histories for the maximum cable tension (i.e., anywhere along the extended cable) and the aircraft angle-of-attack. Cable tension averages about 650 lbf and is never slack, except possibly in the turns, which are omitted from the flight simulations. The cable tension is seen to resonate occasionally (e.g., during the 10th and 11th hours) apparently due to interaction of the cable dynamics and the wind turbine response, and can be addressed by future improvements to the controls logic. The SAIL angle-of-attack is often near the allowable maximum limits since this aircraft must provide lift for both aircraft and a forward aerodynamic thrust. The BOARD angle-of-attack averages near 0°, but produces substantial lift for directional control.
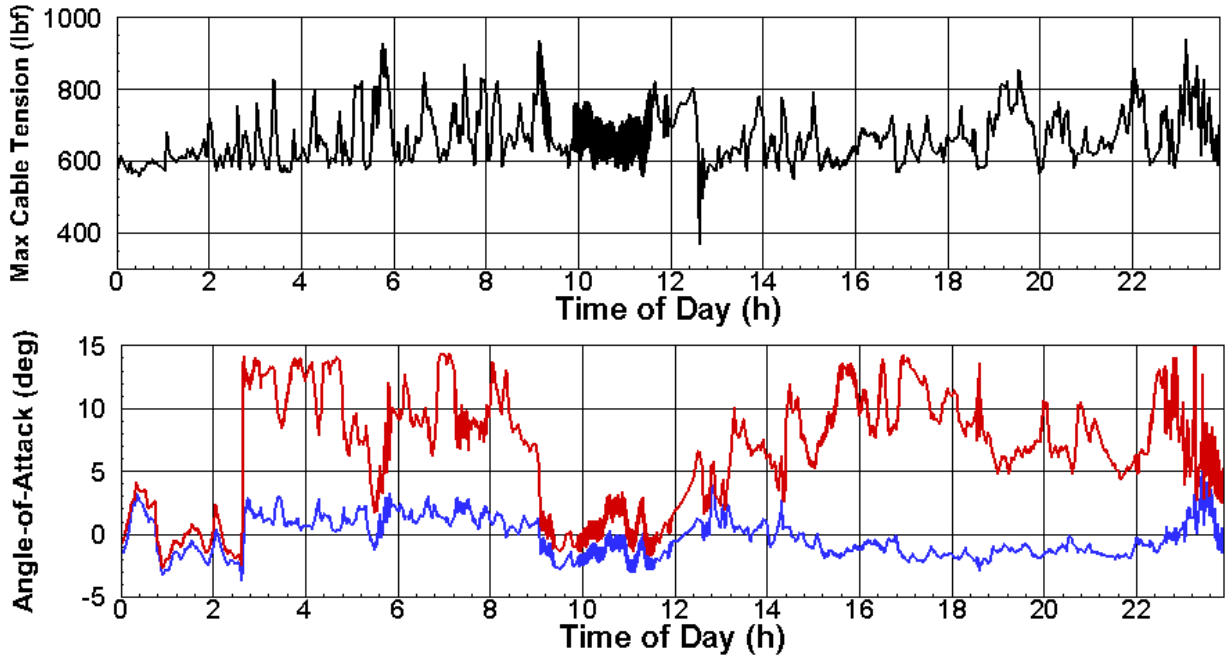
Figure 14. Trajectory histories for maximum cable tension and aircraft angle-of-attack during day #36

Figure 15 illustrates the corresponding DAP ground track for the 24 hour period. The turns that are evident in Figure 12 (roll orientation) are identified in the ground track. The guidance algorithm is currently set to turn around well before the 150-mile boundary if sailing mode conditions are available, as observed in three of the turns in Figure 15, but occasionally is required to turn when the 150-mile boundary is violated regardless of whether sailing mode conditions are available (see turn #4).
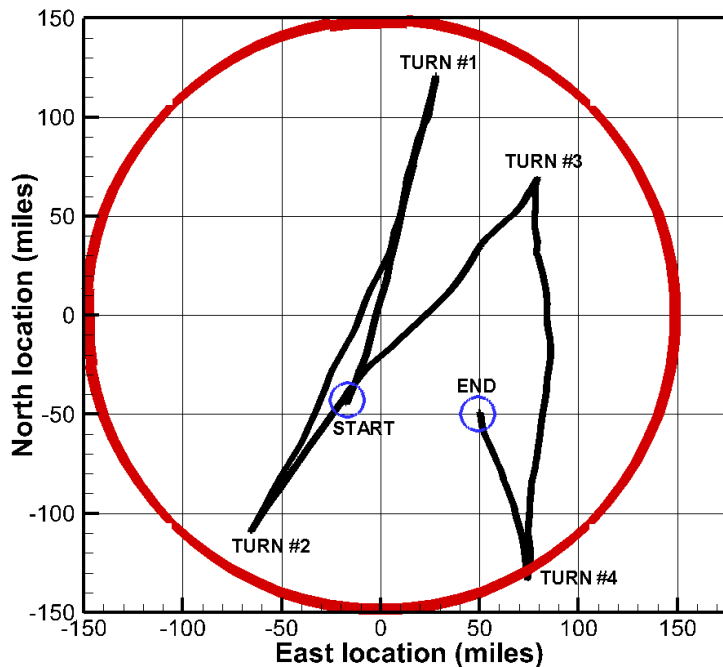

Figure 17. Ground track during day #36 (downtown Orlando at origin)

Conclusions

The DAP concept appears to be potentially viable alternative to the pure solar aircraft for the role of an atmospheric satellite, including as a communications relay over central Florida. Flight dynamics simulation using a detailed transient atmospheric model show that, with accurate LiDAR forecasting of wind profiles, the platform could remain in sailing mode for the vast majority of a long duration mission, greatly reducing the need for propulsion, compared to a pure solar aircraft. Additionally, the flight simulation results show that the SAIL and BOARD aircraft can simultaneously collect significantly more solar energy than the pure solar aircraft. The latter is related to the advantageous use of solar cells/film on both the upper and lower surfaces of the aircraft wings. Since no effort was made in the guidance software to improve solar capture while sailing, further development of the guidance software is expected to further improve net energy available to the payload.

Acknowledgements

References

1. Engblom, W., *Development of Atmospheric Satellite Concept based on Sailing*, AIAA-2012-3203, Applied Aerodynamics Conference, AIAA-2014-1111, AIAA SciTech 2014, Jan 2014.
2. Engblom, W., *Dual-Aircraft Atmospheric Platform*, U.S. Patent Application No. 13/414,451, March 17, 2012.
3. Engblom et al, *Virtual Flight Demonstration of the Stratospheric Dual-Aircraft Platform*, NIAC Phase I Report, 2016.
4. Gentry, B., et al*, Flight Testing of the TWiLiTE Airborne Molecular Doppler Lidar,* International Laser Radiation Conference, St. Petersburg, Russia, Jul. 2010.
5. Kavaya, M., *The Doppler Aerosol Wind (DAWN) Airborne, Wind-Profiling Coherent-Detection Lidar System: Overview and Preliminary Flight Results*, Journal of Atmospheric and Oceanic Technology, 31.4, Apr 2014, 826-842.
6. Amzajerdian, F., Pierrottet, D., "Fiber-based Coherent Lidar for Target Ranging, Velocimetry, and Atmospheric Wind Sensing," Conference on Lasers and Electro-Optics; 21-26 May 2006; Long Beach.
7. Wie, B., *Space Vehicle Dynamics and Control*, 2nd edition, AIAA Education Series, 2008, p. 825.
8. Jackson, E. B., "Manual for a Workstation-based Generic Flight Simulation Program (LaRCsim) Version 1.4," NASA TM-110164, May 1995.
9. Hoerner, *Fluid Dynamic Lift*," 1965 edition, published by author, Chapter 19, p. 9-10.